

# Validation of dynamic RADIANCE-based daylight simulations for a test office with external blinds

Christoph F. Reinhart<sup>\*</sup>, Oliver Walkenhorst

*Solar Building Design Group, Fraunhofer Institute for Solar Energy Systems, Oltmannsstrasse 5, 79100 Freiburg, Germany*

Received 2 August 2000; accepted 2 January 2001

---

## Abstract

The study encompasses the validation of the dynamic, RADIANCE-based daylight simulation method DAYSIM, which uses the concept of daylight coefficients and the Perez sky model to predict the short-time-step development of indoor illuminances. Measured and simulated illuminances have been compared under 10,097 sky conditions in a full-scale test office with a double glazing and external venetian blinds. The additional planning effort for the designer compared to a conventional daylight simulation is addressed. It has been found that the treatment of direct sunlight strongly influences the accuracy of the daylight coefficient method. Three different simulation modes for the direct sunlight are investigated. The simulation results prove that indoor illuminances can be modeled with comparable accuracy for various blind settings under arbitrary sky conditions. Daylight autonomies are predicted with an accuracy below 2% points, where simulation errors stem with roughly equal parts from the raytracing and the sky model. © 2001 Elsevier Science B.V. All rights reserved.

**Keywords:** Commercial buildings; Energy; Comfort; Climate; Dynamic daylight simulations; Daylight coefficients; RADIANCE validation

---

## 1. Introduction

Daylighting, the immediate exploitation of solar energy, forms an established part in the integral design process of a building. It strives to optimize the availability of glare-free, natural daylight to light the interior of a building. The term is predominantly used in the context of commercial buildings in which the times of daylight availability and building occupation largely overlap. The benefits of a carefully planned daylighting concept range from an enhanced visual comfort for the inhabitants to a reduced artificial lighting consumption. As natural daylight is extremely dynamic and cannot be stored, the realization of a suitable daylighting concept involves the assessment of the annual short-time-step development of indoor illuminances at an early design stage. Such indoor illuminance profiles depend on both the building design and the climatic boundary conditions and may serve as a basis to:

- estimate the artificial lighting consumption in a building;
- model further interactions of the daylighting concept with the HVAC system or;
- predict how the overall daylight situation might be perceived by the users.

The latter point highly depends on the users' assigned tasks as well as their subjective and culturally motivated preferences.

The present paper discusses how well the dynamic daylight simulation method, which has been introduced by Reinhart and Herkel [1], is able to model the short-time-step dynamics of the indoor illuminance distribution in a full-scale test office based on direct and diffuse irradiances. The method is termed DAYSIM in the following. DAYSIM is a RADIANCE-based [2] daylight simulation tool which uses the concept of daylight coefficients according to Tregenza [3] and the Perez sky luminance model [4,5] to simulate indoor illuminances under arbitrary sky conditions. RADIANCE is a backward raytracer which blends deterministic and stochastic raytracing techniques [2]. The program has been developed by Greg Ward at Lawrence Berkeley National Laboratories<sup>1</sup> and yields physically based simulations of indoor illuminance and luminance distributions for diffuse, specular and partly specular material surfaces [6]. Even though RADIANCE has been originally designed to model illuminances under a single sky condition, several attempts have been made to predict indoor illuminances under multiple sky conditions [1]. While it has been shown [1] that DAYSIM outperforms several other dynamic

---

<sup>\*</sup> Corresponding author. Tel.: +1-613-993-9703; fax: +1-613-954-3733  
E-mail address: [christoph.reinhart@nrc.ca](mailto:christoph.reinhart@nrc.ca) (C.F. Reinhart).

<sup>1</sup> Source code and binaries can be downloaded for free from the official RADIANCE web side <http://radsite.lbl.gov/radiance/>.

simulation methods in the required simulation times and accuracies, this study concentrates on the validation of simulation results against reality. Therefore, measurements of outdoor direct and diffuse irradiances have been taken synchronously with indoor illuminances in a full-scale test office in 30 s intervals. The facade of the test office featured a double glazing and outer venetian blinds (Fig. 1(a)). The goal was to reproduce measured indoor illuminances based

on outside direct and diffuse irradiances under a wide range of sky conditions and under three different settings of the external venetian blinds. Over 80,000 indoor illuminances have been collected under more than 10,000 sky conditions.

The venetian blind system has been chosen for this study since it is a widely used, multi-functional device which serves as a glare protection, a barrier to unwanted solar gains and a versatile daylighting element to redirect direct sunlight deeper into the room. Apart from its significance as a versatile daylighting element, the venetian blind system is computationally challenging as it requires the simulation of multi-reflected rays.<sup>2</sup>

Mardaljevic has presented a validation of RADIANCE-based indoor illuminance simulations, in which he used sky scanner data to describe the luminance distribution of the celestial hemisphere including the sun [7,8]. In both studies, a new raytracing run was started for each investigated sky condition and the simulation results show how well the RADIANCE raytracing algorithm can model indoor illuminances under perfectly controlled sky conditions. Investigated facade variants encompassed a double glazing and an inner lightshelf with either a diffuse or a partly specular surface and a gray tinted solar control glazing. In contrast to the aforementioned work, the present study aims to:

- validate a dynamic, RADIANCE-based daylight simulation method, DAYSIM, that can efficiently simulate indoor illuminances under arbitrary sky conditions, once a complete set of daylight coefficients for a point in a building has been calculated;
- base daylight simulations on widely available input parameters like direct and diffuse irradiances instead of sky scanner data of the celestial hemisphere;
- investigate a more advanced daylighting element.

Accordingly, our simulation results do not reflect how well a RADIANCE-based daylight simulation can possibly reproduce reality, but provide an estimate of how well a lighting engineer or architect can expect to predict the annual indoor illuminance distribution in a real-world project based on the building geometry, optical properties of the material surfaces and direct and diffuse irradiances. Simulation errors arise from the shortcomings of the Perez sky luminance distribution model, the newly developed daylight coefficient method, the RADIANCE raytracing calculation and the CAD model of the building. The authors are aware that a number of simulation error sources have been avoided in this study, which can further limit the reliability of a daylight simulation. Among them are:

- modeling errors introduced in the process of generating short-time-step irradiance data from hourly or monthly mean values if no measured values are available;

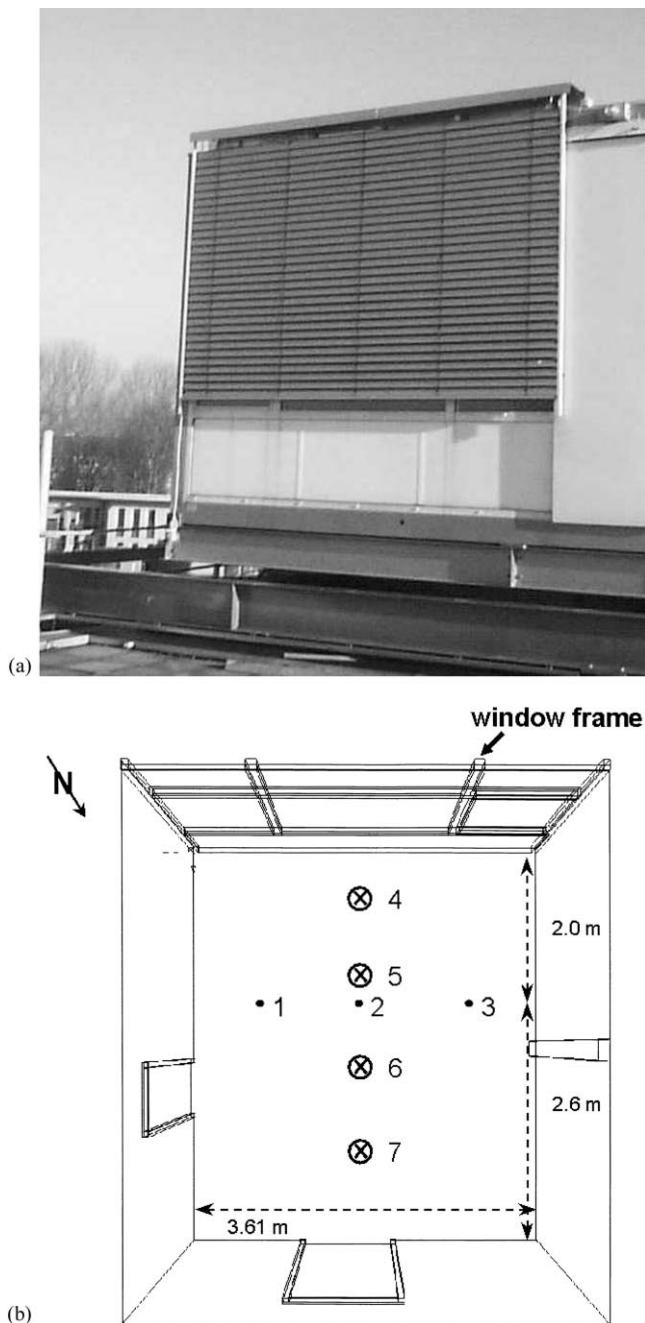


Fig. 1. (a) Photo of the full-scale test office with the blinds closed; (b) sketch of the investigated test office and the sensor positions. Sensors 1–3 are at work plane height (85 cm) facing upwards while the remaining sensors are ceiling mounted facing downwards.

<sup>2</sup>Optical paths which involve multi-reflected beams are difficult to detect for a backward raytracer, as a rising number of inter-reflections between a sensor point and a light source diminishes the chances that a specific path is found.

- the deterioration of material surfaces with time;
- simplification errors in the CAD model of a complex building (construction details, furniture, plants, etc.).

The measurement set-up is presented in Section 2 followed by a description of the daylight coefficient method used by DAYSIM in Section 3. An analysis of the simulation and measurement results is given in Section 4 and summarized in Section 5.

## 2. Experimental set-up

All indoor illuminance measurements were taken in January 2000 at the Fraunhofer Institute for Solar Energy Systems in Freiburg, Germany. The measurements were recorded at several points in a full-scale test office in 30 s intervals with a Hagner detector SD2 in combination with a Keithley multimeter. Each recorded value is the mean of three measurements taken in 10 s intervals. Fig. 1(a) shows the full-scale test office with the outer venetian blinds closed. Room dimensions and the positions of the seven indoor illuminance sensors are shown in Fig. 1(b). Sensors 1–3 were mounted at work plane height (85 cm above the floor) facing up at a 2 m distance from the facade which was facing southwest. Sensor 8 (not shown in Fig. 1(b)) measures vertical illuminances perpendicular to the facade. Sensors 4–7 are ceiling mounted facing downwards. Outside direct normal and diffuse horizontal irradiances as well as horizontal and vertical north, south, east and west illuminances have been collected in 10 s intervals since 1997 [9]. The direct irradiances are measured with an Eppley NIP, while diffuse irradiances are taken with a Kipp & Zonen CM 11 pyranometer. Both measurement devices are mounted on a

2AP tracker. Horizontal and vertical outdoor illuminances are recorded with an LMT illuminance measuring unit and a Licor LI-210SZ, respectively. The measurement errors for the indoor illuminances and the outdoor irradiances are estimated to be 5 and 10%, respectively [10].

Three blind settings were investigated: blinds retracted, blinds down and slat angle in horizontal position and blinds down and slats fully closed, tilted downwards. For all three blind settings, completely and partly overcast as well as sunny sky conditions were recorded and simulated.

## 3. Simulation method

DAYSIM is based on daylight coefficients which are reviewed in the following. For a point and orientation  $x$ , a daylight coefficient  $DC_\alpha(x)$ , related to the sky segment  $S_\alpha$  is defined as the illuminance  $E_\alpha(x)$  at  $x$  caused by the sky segment  $S_\alpha$  divided by the luminance  $L_\alpha$  and the angular size  $\Delta S_\alpha$  of the sky segment (Fig. 2).

$$DC_\alpha(x) = \frac{E_\alpha(x)}{L_\alpha \Delta S_\alpha} \quad (1)$$

A complete set of daylight coefficients can be coupled with an arbitrary sky luminance distribution  $L_\alpha$  ( $\alpha = 1, \dots, N$ ), by a simple linear superposition to calculate the total illuminance  $E(x)$  at  $x$ .

$$E(x) = \sum_{\alpha=1}^N DC_\alpha(x) L_\alpha \Delta S_\alpha \quad (2)$$

Daylight coefficient methods differ in how the celestial hemisphere is divided into disjoint sky segments and how direct sunlight and diffuse daylight are treated. DAYSIM

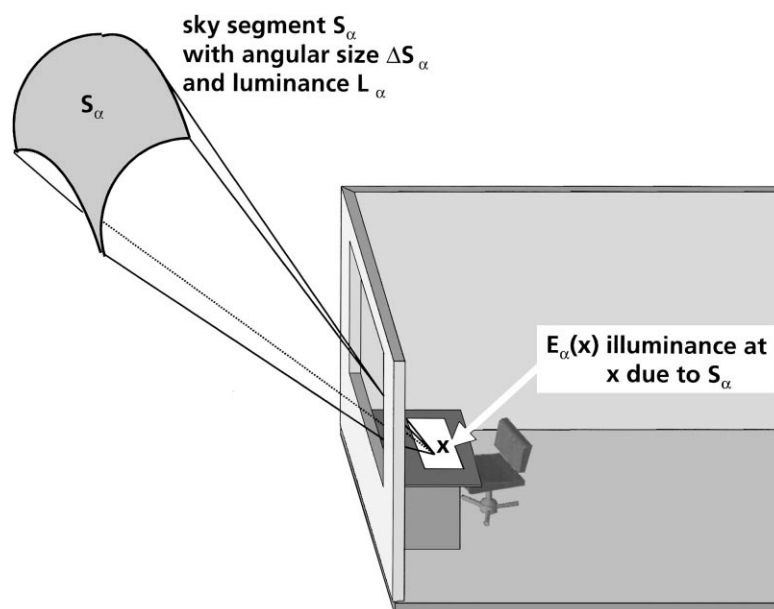


Fig. 2. Graphical definition of a daylight coefficient  $DC_\alpha(x)$  for a point and orientation  $x$ .

distinguishes between contributions from the diffuse daylight, ground reflections and direct sunlight.

$$E(x) = \underbrace{\sum_{\alpha=1}^{145} DC_{\alpha}^{\text{diffuse}}(x) L_{\alpha}^{\text{diffuse}} \Delta S_{\alpha}^{\text{diffuse}}}_{\text{diffuse daylight}} + \underbrace{\sum_{\alpha=1}^3 DC_{\alpha}^{\text{ground}}(x) L_{\alpha}^{\text{ground}} \Delta S_{\alpha}^{\text{ground}}}_{\text{ground reflection}} + \underbrace{\sum_{\alpha=1}^{65} DC_{\alpha}^{\text{direct}}(x) L_{\alpha}^{\text{direct}} \Delta S_{\alpha}^{\text{direct}}}_{\text{direct sunlight}} \quad (3)$$

The celestial hemisphere is divided into 145 sky segments according to the Tregenza division [11] for the diffuse daylight coefficients and three ground segments according to Reinhart and Herkel [1] for the ground daylight coefficients. The number of direct daylight coefficients is site dependent as explained below. For Freiburg, Germany (latitude 47.98°N), 65 direct daylight coefficients are considered. The daylight coefficients are calculated with an adapted version of the RADIANCE version 3.1.8 [2]. Details are provided in the Appendix A.

Fig. 3 shows a flow diagram of a DAYSIM simulation. Inputs are the regular RADIANCE geometry and material input files, RADIANCE simulation parameters, building site coordinates and a time series of direct and diffuse irradiances. In a first simulation step, a whole set of 145 diffuse, three ground and 65 direct daylight coefficients is calculated for all points of interest in a building. Afterwards, the sky luminances pertaining to the daylight coefficients are calculated using the Perez sky model according to the selected assignment mode (see below). The resulting luminances are

coupled with the daylight coefficients according to Eq. (3). Sections 3.1 and 3.2 describe how DAYSIM divides the sky into disjoint segments and how the sky luminances are assigned to the different daylight coefficients.

### 3.1. Diffuse daylight and ground reflections

The luminances of the 145 diffuse sky segments for a particular sky condition are calculated with the Perez all weather sky model [4,5] based on date and time as well as on direct normal and diffuse horizontal irradiances. The diffuse luminance,  $L_{\alpha}^{\text{diffuse}}$ , of a particular sky segment is set equal to the value of the Perez sky luminance distribution function at the center of the sky segment. The luminances pertaining to the three ground daylight coefficients are modeled according to the RADIANCE program *gendaylit* [12].

### 3.2. Direct sunlight

Contributions from direct sunlight are modeled by some 65 representative sun positions, which are a subset of all possible sun positions throughout the year. Fig. 4 shows all annual hourly mean sun positions (dots) for Freiburg, Germany, together with the 65 representative sun positions (crosses) for which direct daylight coefficients are calculated. The representative sun positions correspond to the actual sun positions on all full-hour solar times for the 21st of December, February/October, March/September, April/August and June at which the sun is above the horizon. Accordingly, the four direct daylight coefficients surrounded by the box in Fig. 4 correspond to the actual sun positions in Freiburg on 21st June and 21st April/August at 13.00 and 14.00 solar time. At sunrise and sunset the direct daylight coefficients correspond to the solar time with a solar altitude of 2°, so that low solar altitudes can be correctly modeled.

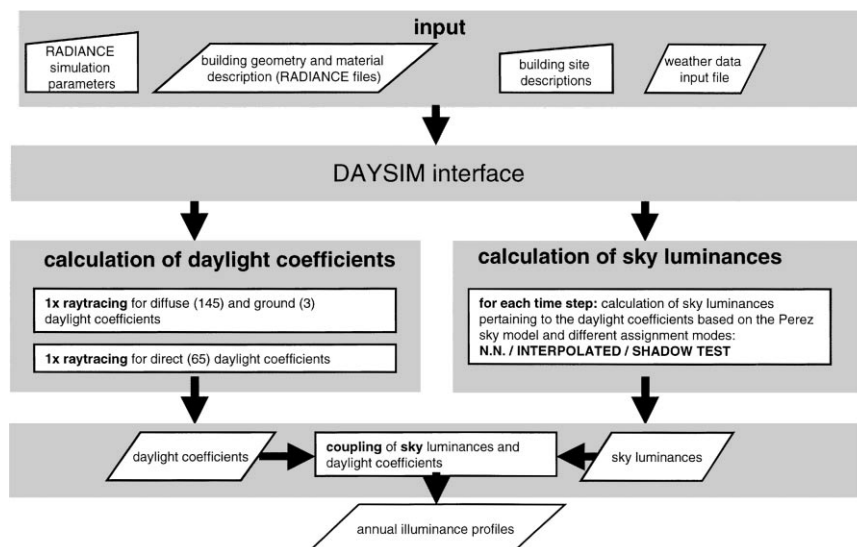


Fig. 3. Flow diagram of the simulation method DAYSIM.

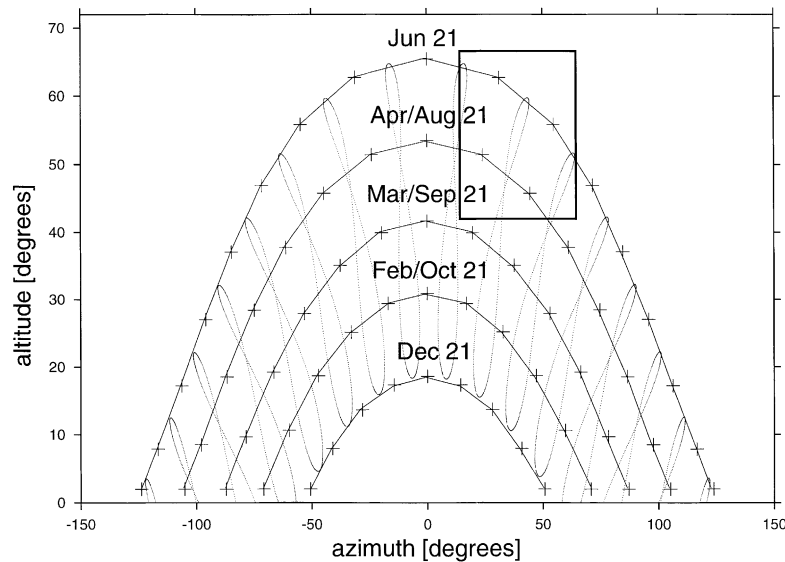


Fig. 4. The dots mark all annual hourly mean sun positions for Freiburg, Germany (47.979°N); the crosses mark the 65 representative sun positions for which direct daylight coefficients are calculated. The box in the upper part of the figure surrounds four representative sun positions which correspond to actual sun positions at 13.00 and 14.00 solar time on 21st June and 21st April/August.

The total number of direct daylight coefficients is site dependent and varies from 61 to 65 for latitudes below 70°. Near the poles the number decreases down to 48.

The assignment of the direct luminances,  $L_{\alpha}^{\text{direct}}$  ( $\alpha = 1, \dots, 65$ ), for a given sky condition is not as unambiguous as for the diffuse illuminances. Three assignment modes have been tested.

1. NEAREST NEIGHBOR (NN): the simplest method is to completely assign the luminance from the sun,  $L^{\text{sun}}$ , for a given sky condition to the representative sun position, which lies closest to the actual sun position in the altitude-azimuth plane, i.e.  $L_{\alpha=\text{NN}}^{\text{direct}} = L^{\text{sun}}$ . The luminances of the remaining representative sun positions are set to zero (Fig. 5(a)).
2. INTERPOLATED: a more sophisticated method is to pick for a given date and time the four representative sun positions which surround the actual sun position (Fig. 5(b)). The luminance from the sun,  $L^{\text{sun}}$ , is distributed among these four daylight coefficients according to a weight, which considers the time and solar altitude of the actual and the four picked representative sun positions. This two-fold division is exemplified in Fig. 5(b). The actual sun position corresponds to 13.25 solar time on 7th May. The actual solar altitude is 54°. The weight assigned to the two representative sun positions at 13.00 solar time and the two sun positions at 14.00 solar time is divided according to the fraction 25:35. The two sun position pairs on 21st June and 21st April/August are weighted according to the altitude difference fraction of the actual altitude and the solar altitudes on these dates at 13.25 solar time: 60° for 21st June and 49° for 21st April/August. Accordingly, the direct luminance assigned to

the representative sun position at 13.00 solar time on 21st June is 27%.<sup>3</sup> The weights assigned to the other three surrounding representative sun positions are shown in Fig. 5(b). The luminances of the 61 remaining representative sun positions are set to zero.

3. SHADOW TEST: a shortcoming of the two above described algorithms is that in case the point of interest in the building,  $x$ , lies in direct view of the actual sun position, while the position of one or several of the surrounding representative sun positions is shaded or vice versa, the assignment of direct luminances to these representative sun positions is not suitable to model the indoor illuminance at  $x$  for the investigated actual sun position. To avoid this problem, INTERPOLATED can be coupled with a simple shadow testing procedure: an initial shadow testing<sup>4</sup> notes for each representative sun position, whether  $x$  lies in its direct view (direct view = 1) or not (direct view = 0). For a given sky condition only those surrounding representative sun positions are considered whose direct view status equals the status of the actual sun position. In Fig. 5(c), the two representative sun positions corresponding to 21st April/August cannot be seen from  $x$  opposed to the actual sun position. Therefore, the direct solar luminance is assigned to the remaining two representative sun positions. SHADOW TEST runs into problems if all surrounding representative sun positions are shaded, while the actual sun position is not or vice versa. In this case, a warning is generated for the considered time step and the direct contribution is set to zero. During the

<sup>3</sup>  $100\% \times (35 \text{ min}/60 \text{ min}) \times [(54-49)/(60-49)]$ .

<sup>4</sup> A shadow testing involves the backward tracing of a single ray to test whether a point can be directly illuminated by a light source.

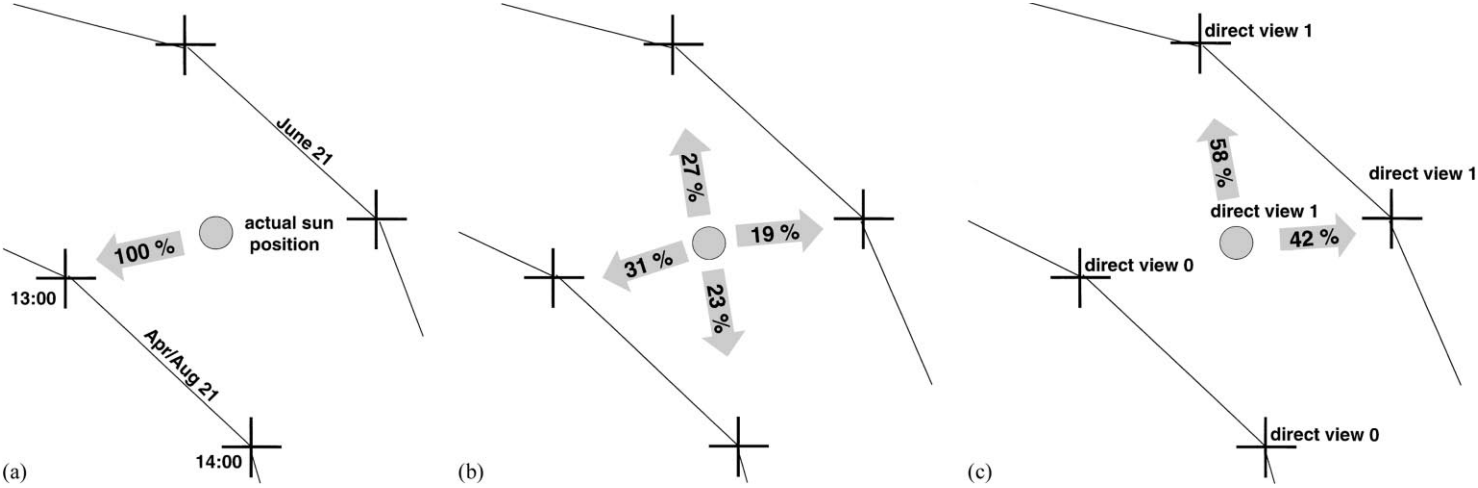


Fig. 5. Visualization of the three investigated assignment modes of direct solar luminances to the representative sun positions. The four representative sun positions correspond to the ones in the box in Fig. 4: (a) NN; (b) INTERPOLATED; (c) SHADOW TEST.

simulations for this study, this problem appeared in 10 out of 70,679 indoor illuminance simulations for all the sky conditions, blind settings and sensor positions. If this problem should become more urgent for a particular building design, the number of representative sun positions can be enlarged at the expense of longer calculation times.

The performance of the three assignment modes is discussed in Section 4.

### 3.3. Simulation inputs

As shown in Fig. 3, DAYSIM requires measured direct and diffuse irradiances as well as the test office geometry and material surfaces as simulation inputs. The geometry of the full-scale test room was modeled with an accuracy of  $\pm 2$  cm. According to Wienold et al. [10], the walls, the ceiling and the floor of the test room can be treated like perfectly Lambertian surfaces. The reflectances have been taken from Wienold et al. [10]. The direct hemispherical visible transmittance of the double glazing was 79% which corresponds to a transmissivity of 87.6%<sup>5</sup> [6]. The optical surface properties of the gray metallic outer blinds has been characterized with an integrating sphere. The test office is situated on the roof of the Fraunhofer Institute for Solar Energy Systems. It has been found that the reflectivity of the roof is a crucial simulation input parameter, as it nearly directly scales with the daylight that is seen by the ceiling sensors. The roof was modeled purely Lambertian with a reflectivity of 5%. The remaining ground albedo was assigned a reflectivity of 20%.

Indoor illuminances at the seven sensor positions shown in Fig. 1(b) were modeled for over 10,000 sky conditions. Only sky conditions with outdoor horizontal illuminances above 1000 lx were considered. All simulations have been carried out with the same set of RADIANCE raytracing parameters on several Pentium Pro 400 MHz Linux workstations with 256MB RAM and a dual processor board. Even though the new method requires additional RAM compared to a conventional *rtrace* run swapping could be avoided during all simulations.

## 4. Results and analysis

### 4.1. Conventional *rtrace* simulations and DAYSIM

Before DAYSIM simulation results are compared to actual measurements, this paragraph weighs the benefits and drawbacks of DAYSIM with respect to a conventional RADIANCE simulation. What are the additional planning

efforts for the designer, the required calculation times, the suitable RADIANCE parameters and the hardware requirements, i.e. what is the price for simulating indoor illuminances under multiple instead of a single sky condition?

- Additional design work: DAYSIM uses the same material and geometry input files as a conventional RADIANCE simulation. This is important as the generation of the CAD model is usually the most time demanding part of a simulation. Direct and diffuse irradiance data are widely available in the form of test reference years (TRY). Therefore, the additional design effort for running an annual daylight simulation is usually small and, as DAYSIM has been widely automated, mainly requires additional CPU time.
- Calculation times: Fig. 6 compares calculation times for the three investigated blind settings for a single sky condition with direct sunlight and for a complete set of daylight coefficients. Shown are the ratios of the calculation times for arbitrary sky conditions to a single sky condition. The actual calculation times are printed above the columns. While the ratio lies around 8 for retracted blinds, it drops below 5 for closed blinds. This indicates that the significance of the daylight-coefficient-specific contribution to the overall calculation falls with growing complexity of the raytracing calculation.
- RADIANCE parameters: a chosen set of raytracing parameters decisively influences the accuracy of a simulation and its calculation time. Therefore, the accuracy of simulation results for conventional RADIANCE and DAYSIM have been compared to various sets of raytracing

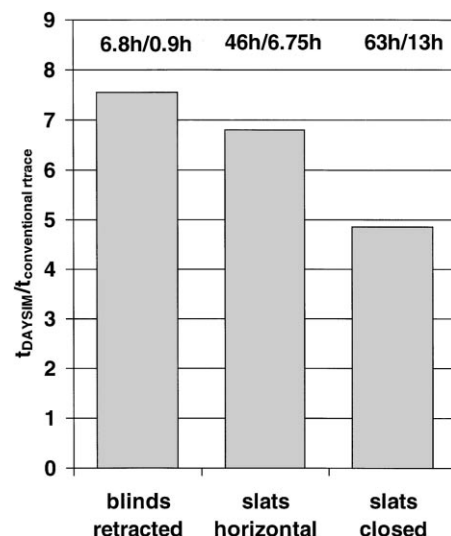


Fig. 6. Comparison of the ratios of the necessary calculation times for a DAYSIM simulation which yields a complete set of daylight coefficients to a conventional RADIANCE simulation. All calculations involved the simulation of illuminances for seven points inside the test office. Actual calculation times are printed above the columns. The ratios fall with rising model complexity.

<sup>5</sup> The transmissivity is a theoretical value which specifies the amount of light that penetrates a surface excluding inter-reflections ([6] p. 239). It is the input parameter to model glazings with RADIANCE.

parameters. The results were that the same set of simulation parameters yields very similar accuracies for both methods under various sky conditions and blind settings. Differences mainly arise under sunny sky conditions as DAYSIM has to estimate contributions from the direct sunlight from the available representative sun positions. This important finding implies that the same set of RADIANCE parameters can be used for a dynamic daylight simulation as for the simulation of a single sky condition. Again, no additional effort for the designer is required.

- Hardware requirements: as explained in the Appendix A, the adapted *rtrace*-version demands about eight times more RAM than a conventional *rtrace* simulation due to extended caching information. In the times of continuously rising hardware capabilities, the 256MB RAM used for all simulations in this study should not constitute a severe financial barrier for a potential user of the simulation method.

#### 4.2. Overcast sky conditions

The following paragraph discusses how well DAYSIM performs on cloudy days. Fig. 7(a) presents measured and simulated<sup>6</sup> outdoor horizontal illuminances for the 7th of January 2000, an overcast day with varying cloud cover thickness. Measured and simulated results basically coincide throughout the day. Fig. 7(b) shows measured and simulated vertical illuminances on the southwestern facade of the test office for the same day. Errors in the sky luminance distribution model are clearly visible especially when the cloud cover is thin. In Fig. 7(c), measured and simulated horizontal illuminances are plotted for sensor #2 (see Fig. 1(b)) in the test office. The blinds were retracted on this day. The simulated values are close to the measured values for most of the day. To be able to distinguish between simulation errors due to the sky model and the raytracing algorithm, an additional variant, 'scaled', is plotted in Fig. 7(c). For this variant the simulated illuminances are multiplied with the ratio of the measured to the simulated facade illuminances from Fig. 7(b). The corrected simulation results and the indoor measurements basically coincide throughout the day. This reveals that for such a straightforward building geometry most simulation errors can be attributed to the sky model.

Fig. 7(d) and (e) present measured and simulated illuminances for sensor #2 with the blinds closed and slat angles horizontal and tilted downwards, respectively. Note how well the simulated illuminances approach the measured values even for this challenging daylighting element under cloudy sky conditions. Scaling the data as in Fig. 7(c) did not significantly improve the simulation results. A reason for this might be that scaling simulation results corrects

for errors of the sky luminance distribution. As indoor illuminances behind closed blinds arise from daylight that is reflected from the surrounding ground, the significance of the sky luminance distribution model falls for such facade geometries.

A comparison of the different ceiling mounted sensors revealed that the sensor closest to the facade was modeled with the lowest accuracy for all blind settings and sky conditions. Obviously, this sensor is strongly influenced by the surrounding landscape which could not be modeled as precisely as the remaining test office.

#### 4.3. Sunny sky conditions

The situation is more complicated for sunny sky conditions. Fig. 8(a) shows simulated and measured outside horizontal illuminances for a sunny day for two assignment modes, INTERPOLATED and NN. INTERPOLATED approaches the measured values very well, while NN introduces a step-like behavior in the temporal development of the illuminances. The discontinuities appear when the nearest representative sun position changes. Fig. 8(b) presents indoor illuminances for sensor #2 on the morning of 8th January. The step-like behavior of the NN plot is even more pronounced than for the outside horizontal case. This suggests that the method is not apt to model the short-time-steps dynamics inside a building with sufficient detail. The remaining paragraph concentrates on the INTERPOLATED and SHADOW TEST modes.

While SHADOW TEST does not differ from INTERPOLATED for an unshaded point, Fig. 8(c) pictures its advantage for the indoor sensor #2 on a sunny day. At 14.15 measured and SHADOW TEST illuminances abruptly fall as the sensor is temporarily shaded from direct sunlight by the window frame marked in Fig. 1(b). Such details in the temporal development of the indoor illuminance cannot be detected by INTERPOLATED. Fig. 8(d) shows the situation for the same sensor with the blinds closed and the slats in horizontal position. The measured illuminances exhibit sharp illuminance variations throughout the day as soon as direct light enters the room due to the single slats. SHADOW TEST exactly reproduces these variations while INTERPOLATED fails to model them. If an investigated point is subject to direct sunlight SHADOW TEST is superior to INTERPOLATED, as it may help to predict the appearance of glare as well as irritating abrupt illuminance variations.

Fig. 8(e) provides an impression of how the various assignment modes perform under sunny sky conditions with the blinds fully closed. The bump of INTERPOLATED at 16.00 comes about as one of the representative sun positions lay in direct view of the sensor, even with the blinds fully closed. This was possible since the closed venetian blinds left about 10 cm of the glazing uncovered. As the sensor has never really been directly illuminated by the sun on this day, SHADOW TEST eliminates such simulation errors.

<sup>6</sup>For overcast sky conditions all three direct assignment modes yield the same results.



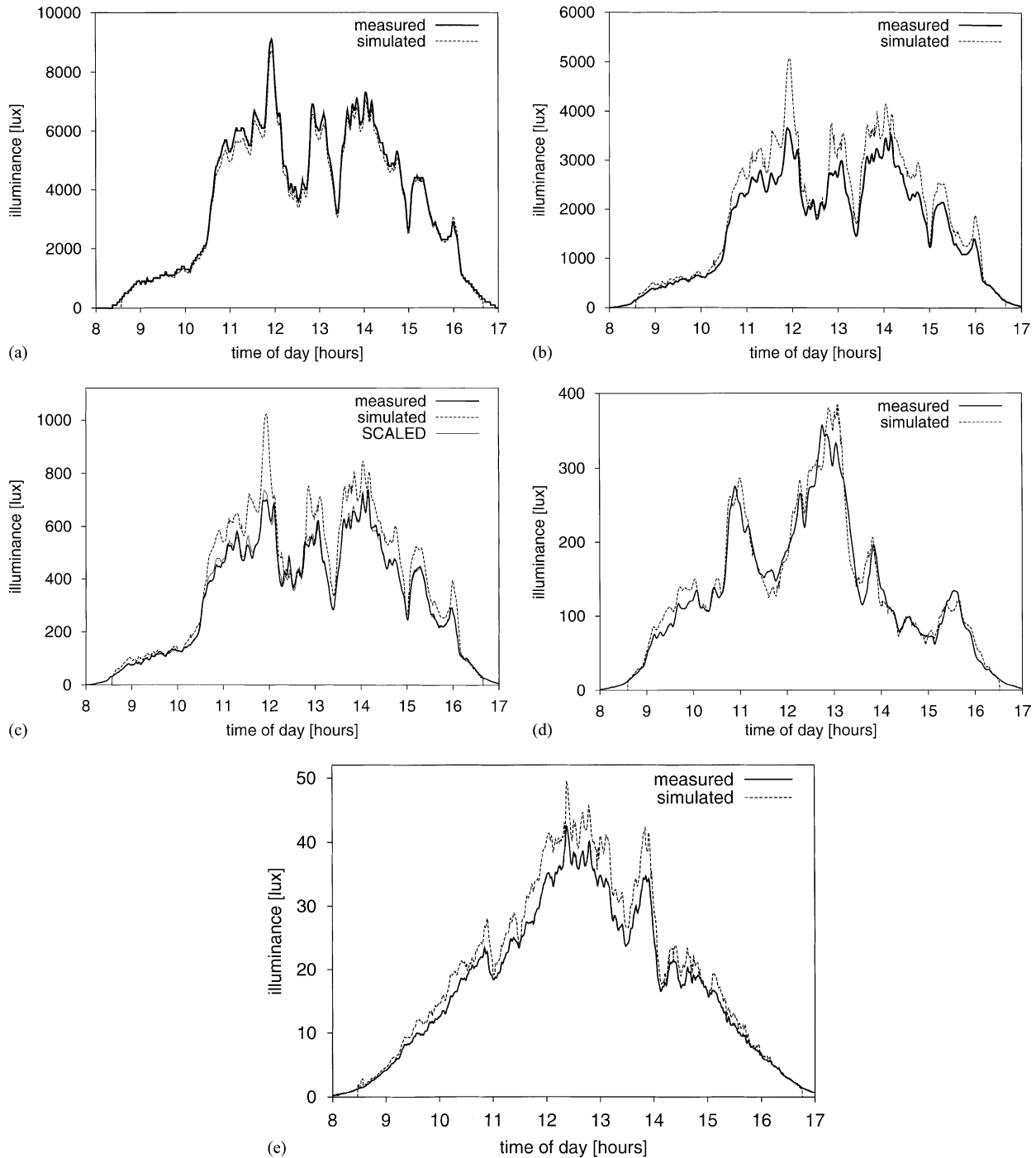


Fig. 7. Cloudy sky conditions: (a) measured and simulated outside horizontal illuminances (7th January 2000); (b) measured and simulated vertical illuminances on the facade of the test office (7th January 2000); (c) measured, simulated and 'scaled' horizontal illuminances for sensor #2, the blinds are retracted (7th January 2000); (d) measured and simulated horizontal illuminances for sensor #2, the blinds are down and slats horizontal (11th January 2000); (e) measured and simulated horizontal illuminances for sensor #2, the blinds are down and slats tilted downwards (15th January 2000). Note how well illuminances even below 50 lx can be modeled.

#### 4.4. Arbitrary sky conditions

Table 1 summarizes the simulation errors for all three blind settings for all sky conditions for which indoor illuminances have been measured. The averages of the relative mean bias errors (MBE) and relative root mean squared

errors (RMSE)<sup>7</sup> of the four ceiling and the three desk height sensors are listed separately for all three assignment modes. Only sky conditions with outside horizontal illuminances above 1000 lx were considered.

$${}^7\text{MBE}_{\text{rel}} = \frac{1}{N} \sum_{i=1}^N \frac{x_{\text{sim},i} - x_{\text{mea},i}}{x_{\text{mea},i}}, \quad \text{RMSE}_{\text{rel}} = \frac{1}{N} \sqrt{\sum_{i=1}^N \left( \frac{x_{\text{sim},i} - x_{\text{mea},i}}{x_{\text{mea},i}} \right)^2}.$$

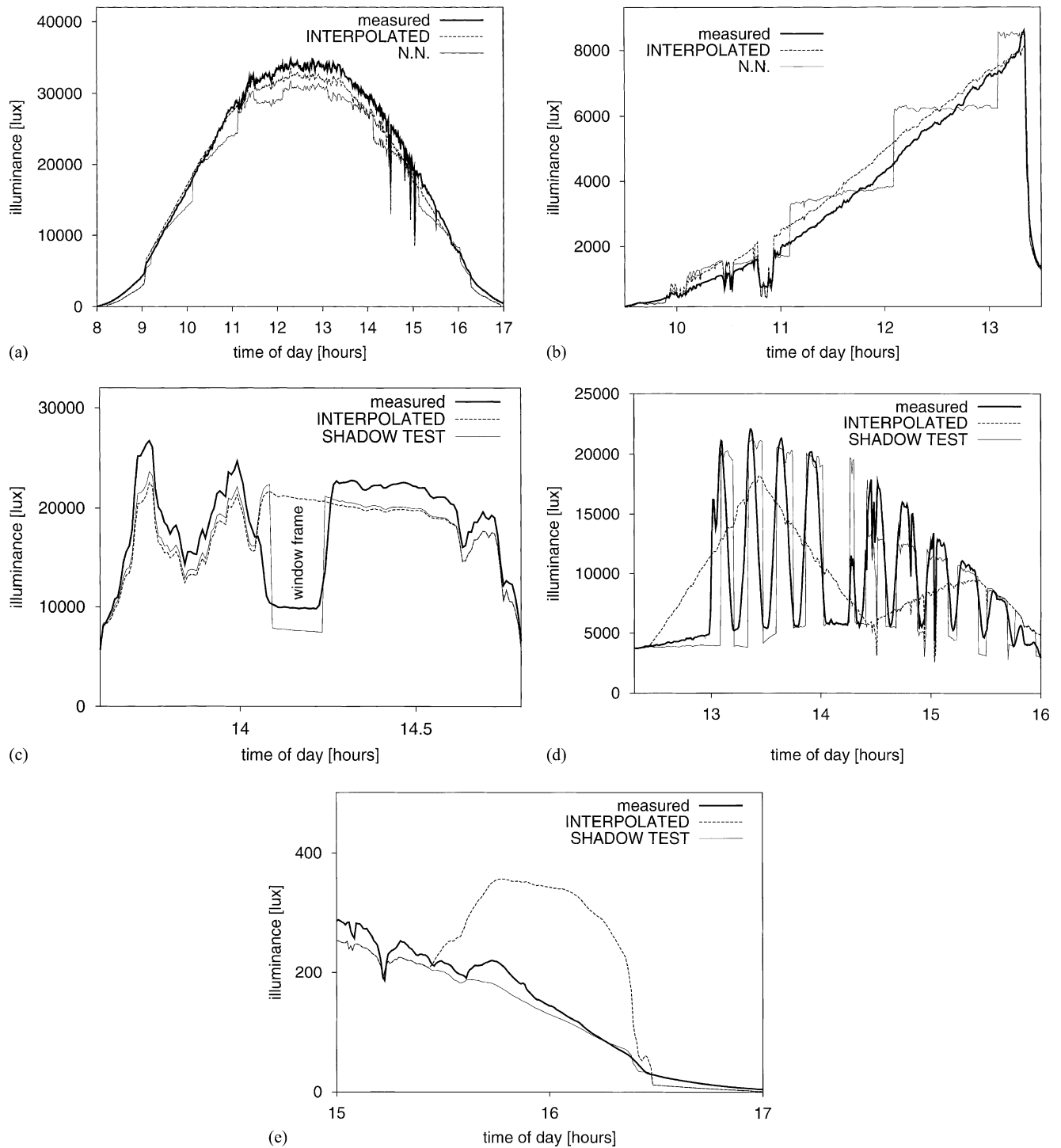


Fig. 8. Sunny sky condition: (a) measured, INTERPOLATED and NN outside horizontal illuminances (13th January 2000). The NN assignment mode introduces a step-like behavior for the outside illuminances. (b) Measured, INTERPOLATED and NN horizontal illuminances for sensor #2 (8th January 2000). The blinds are retracted. The discontinuities introduced by NN are even more pronounced than for the outside case. (c) Measured, INTERPOLATED and SHADOW TEST horizontal illuminances for sensor #2 (6th January 2000). The blinds are retracted. Note how SHADOW TEST detects the window frame while INTERPOLATED skips on this detail. (d) Measured, INTERPOLATED and SHADOW TEST horizontal illuminances for sensor #2 (13th January 2000). The blinds are down with slat angles horizontal. Note how SHADOW TEST simulates the pronounced illuminance variations as the sun moves in and out of direct view of the investigated point. (e) Measured, INTERPOLATED and SHADOW TEST horizontal illuminances for sensor #2 (16th January 2000). The blinds are down with slat tilted downwards. The artifact introduced by INTERPOLATED vanishes due to shadow testing.

Table 1  
Relative RMSE and MBE for the three investigated assignment modes

		Nearest neighbor		Interpolated		Shadow test	
		MBE (%)	RMSE (%)	MBE (%)	RMSE (%)	MBE (%)	RMSE (%)
Blinds retracted	Ceiling	17	30	17	30	17	30
	Desk	6	24	8	24	6	22
Blinds closed, slats horizontal	Ceiling	20	32	20	31	20	31
	Desk	6	29	7	28	5	25
Blind closed, slats tilted downwards	Ceiling	−6	27	−6	26	−6	26
	Desk	−1	30	2	33	−6	24

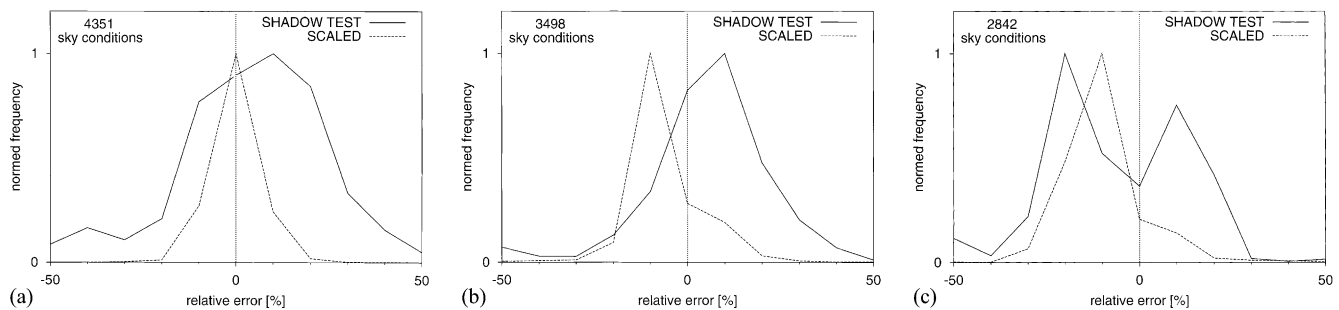


Fig. 9. Frequency distribution of relative errors for sensor #2 for the three investigated blind settings: (a) blinds retracted; (b) horizontal slats; (c) blinds closed.

For the retracted blinds, the MBE and RMSE tend to be higher for the ceiling than for the desk sensors. As mentioned above, the difficulty with the ceiling sensors is that they are strongly influenced by details of the surrounding landscape which usually cannot be modeled. As closed-looped automated control systems for an artificial lighting system often feature ceiling-mounted photosensors, the modeling of the energy performance of such systems would be similarly affected.

The MBE and RMSE are similar for all assignment modes. This finding implies that although NN introduces discontinuities in the time development of indoor illuminances, the overall accuracy of the simulations is not significantly impeded.

For the horizontal slats, the ceiling is modeled with nearly the same accuracy as in the absence of blinds, only the MBE lie about 3% higher. The desk MBE also resemble the ones without blinds. Only the desk RMSE for INTERPOLATED and NN are 4–5% higher than without blinds. These additional errors arise from shortcomings of these assignment modes as explained in Section 4.3 which partly vanish for SHADOW TEST. The effect is more pronounced if only RMSE for sunny sky conditions are considered (direct normal radiation  $> 2 \text{ W/m}^2$ ). For these sky conditions, the average desk RMSE rise from 24 to 40% for INTERPOLATED and NN, while they does not significantly change for SHADOW TEST. It is surprising to realize how little the introduction of horizontal blinds impedes the simulation accuracy of SHADOW TEST even for sunny sky conditions.

For the closed blinds, ceiling MBE and RMSE are again nearly identical for all assignment modes. For SHADOW TEST ceiling and desk errors are roughly identical. This strong coupling of the simulation accuracies for ceiling and desk can be expected for this blind setting as daylight almost exclusively illuminates the desk sensors via reflections from the ceiling.<sup>8</sup> The correlation is not found for INTERPOLATED and NN as the late afternoon simulation artifact shown in Fig. 8(e) appeared every sunny afternoon and increased the desk RMSE. Again, the magnitude of the desk RMSE for SHADOW TEST are about the same size as for the other two blind settings.

Fig. 9 aims to provide some insight into how the total errors from Table 1 can be divided into errors due to the raytracing and to the sky model. The figure presents the frequency distributions of the relative errors of all simulated illuminances at sensor #2 for the three blind settings separately. For the retracted blinds SHADOW TEST has a wide peak and the center of weight lies at 6%. The RMSE for this distribution is 22% (Table 1). After scaling the peak narrows to a RMSE of 10% and shifts to a MBE of 0%. This behavior again proves how exact the raytracing algorithm can model indoor illuminances in the absence of blinds. Our findings for this geometry are in accordance with the results of

<sup>8</sup> When the blinds are lowered with the slats tilted downwards incoming daylight is either multiple-reflected between two slats or directly passes the blinds after a reflection from the external ground. In both cases incoming rays are directed upwards, so that they need to be reflected from the ceiling before they can hit sensor #2.

Mardaljevic [7] who found a MBE of 1% and a RMSE of 17.9% for a point at 2.5 m distance to a facade with a single glazing.

For the horizontal slats the situation is similar: the wide SHADOW TEST peak with an associated RMSE of 25% narrows down to 17% after scaling. The ‘scaled’ peak is not centered around 0% as the sensor is only partly exposed to the celestial hemisphere due to the slats.

For the closed blinds the frequency distribution of SHADOW TEST features two peaks. The higher peak at about 10% stems from the cloudy skies (Fig. 7(e)) while the peak at –20% stems from the sunny skies. The scaling merges the peaks and reduces the RMSE from 24 to 15%. The results for the three blind setting suggest that the simulation errors of DAYSIM stem to roughly equal parts from the raytracing algorithm and the sky model.

#### 4.5. How representative are the measured data?

This study aims to estimate how well the annual indoor daylight availability in the test office can be simulated. As explained above, simulation errors stem from the raytracing calculation as well as from the underlying sky model. Especially for retracted blinds the simulation errors mainly stem from the sky model, i.e. how accurate the illuminance onto the facade is simulated for a given sky condition. As indoor and outdoor illuminance measurements have only been collected for 2 weeks in January 2000 in Freiburg, Germany, a careful analysis has been carried out to test how well the recorded sky conditions can be modeled compared to all appearing sky conditions throughout the year. To this end, simulated horizontal and vertical outside illuminances based on direct and diffuse irradiances have been compared to measured values for the 2-weeks period in January 2000 in 30 s time steps and for the complete year of 1998 in 1 min time steps. The surrounding landscape was considered in the simulations.

Table 2 lists the relative MBE and relative RMSE for the 2 weeks in January 2000 and (in parentheses) the complete year of 1998. Simulation errors are shown for the INTERPOLATED and NN assignment modes. As SHADOW TEST yields identical results as INTERPOLATED for outside

horizontal illuminances and nearly identical results ( $\pm 1\%$ ) for outside vertical illuminances, the simulation results are not listed in Table 2. The table reveals that both considered assignment modes simulate outdoor illuminances for various sky directions with similar accuracy. Differences between the two modes are less or equal to 2% for all orientations.

The MBE and RMSE for global horizontal illuminances for the whole year and for the 2 weeks are nearly identical ( $<2\%$ ), showing that the Perez sky luminous efficacy model yields slightly too low values for the Freiburg climate all year around. The annual RMSE for the vertical sky directions tend to lie below the values for the 2 weeks. Only northern illuminances are slightly better simulated for the 2 weeks than for 1998. The main differences between the two data sets are the MBE for the vertical illuminances which vanish for the whole year while they lie between 4 and 8% for the 2 weeks. The surprising fact that the vertical illuminances tend to be overestimated while horizontal illuminances are slightly underestimated during the 2 weeks hints that the Perez sky luminance distribution sometimes yields too high luminances near the horizon.

The results from Table 2 imply that the sky conditions which have been collected during the 2 weeks can be modeled with an accuracy which is representative for all sky conditions throughout the year. From this information it can be inferred that, at least for retracted blinds, the results from Sections 4.2 to 4.4 can be generalized for arbitrary sky conditions.

#### 4.6. Error analysis for the daylight autonomy and artificial lighting demand

While the relative MBE and RSME are standard statistical measures to express how well a simulation method approaches a reference case, it is difficult to infer from these quantities how well more instructional characteristics of a building design can be modeled by DAYSIM. The daylight autonomy for a point in a building is a useful physical quantity that denotes the fraction of a considered time interval during which a minimum illuminance level can be maintained by daylight alone. Usually the considered

Table 2

Relative MBE and relative RMSE of simulated illuminances for an unshaded point facing up and in the four main sky directions<sup>a</sup>

Outside	Interpolated		Nearest neighbor	
	MBE <sub>rel</sub> (%) (whole year)	RMSE <sub>rel</sub> (%) (whole year)	MBE <sub>rel</sub> (%) (whole year)	RMSE <sub>rel</sub> (%) (whole year)
Horizontal	–6 (–7)	10 (12)	–7 (–7)	12 (12)
North	4 (–1)	17 (19)	4 (–1)	17 (20)
South	5 (3)	24 (21)	6 (2)	24 (22)
West	6 (–1)	21 (20)	5 (–1)	21 (21)
East	7 (0)	23 (21)	8 (0)	25 (21)

<sup>a</sup> The values are based on the 10,097 sky conditions with measured outside horizontal illuminances above 1000 lx for which indoor illuminances have been collected. The values in parentheses are based on measured values for the whole year of 1998 (2,50,196 values). Results are presented for the interpolated and the NN assignment modes.

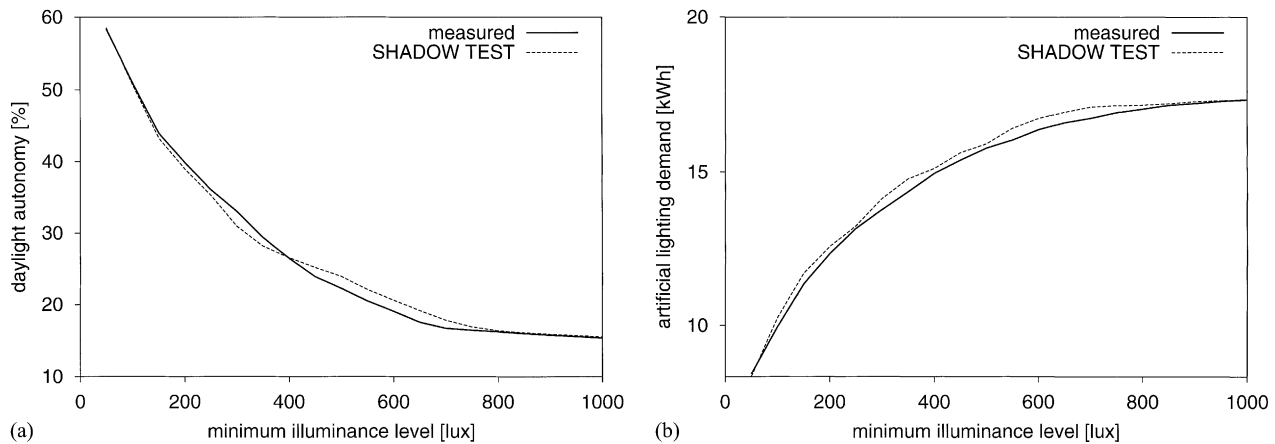


Fig. 10. Measured and simulated (SHADOW TEST) daylight autonomy (a) and artificial lighting demand (b) for the 2-weeks measurement period for a point at 2 m distance from the facade (sensor #2). For the artificial lighting demand an ideal, automated lighting control system has been considered.

time interval corresponds to the hours per year when a work place is occupied. The required minimum illuminance levels range from 150 [13] to more than 1000 lx [14] depending on the applicable legal requirements and the individual user preferences. The daylight autonomy indicates how often artificial lighting can be avoided at a work place. Fig. 10(a) plots measured and simulated daylight autonomies for sensor #2 in the test office for different minimum illuminance levels. The underlying time interval are all hours between 7 a.m. and 6 p.m. during the 2 weeks when indoor illuminances were collected. Fig. 10(a) clearly shows that the simulated and measured daylight autonomies never differ by more than 2% points even though all three blind positions are considered to roughly equal parts.

It has been shown in Section 4.5 that the underlying sky conditions of the daylight autonomies shown in Fig. 10(a) are rather challenging to model compared to all appearing sky conditions of the year. Therefore, it can be inferred that DAYSIM is able to model annual daylight autonomies with a comparable accuracy as in Fig. 10(a).

Whereas the daylight autonomy is a uniquely defined, physical quantity which describes the daylight availability in a building, artificial lighting demand further depends on the installed lighting system as well as occupancy and individual preferences. The task of linking indoor illuminance distributions to artificial lighting demand is a very complicated matter. Nevertheless, the energy demand for an automated, closed loop control strategy has been calculated in Fig. 10(b) based on measured and simulated illuminances for the 2-weeks measurement period. This sample calculation provides a raw estimate of how accurate artificial lighting demand can be predicted for an ideal, fully automated lighting control system. It is assumed that, an ideal closed loop control system switches the artificial lighting in the room if indoor illuminances due to daylight fall below the minimum illuminance threshold. The simulated lighting system has an installed power of 166 W, which corresponds to an installed power per unit area of  $10 \text{ W/m}^2$  in the test box.

If indoor illuminances rise above the threshold, the lighting is automatically switched off once the threshold illuminance has been maintained for more than 15 min. This inertia of the system has been added to reduce the number of distracting, automated switching events.

Fig. 10(b) shows that the artificial lighting demand for the 2-weeks measurement period can be satisfactorily predicted. Again, the reader should bear in mind that the ideal, automated control strategy, which has been considered here, is a very basic model for estimating the artificial lighting demand in an office.

## 5. Discussion and conclusion

The last section covered various performance aspects of DAYSIM including the impact of different assignment modes, blind settings, sky conditions and sensor positions, the simulation accuracy of indoor illuminance levels, daylight autonomies and artificial lighting demands and the handling of the method.

### 5.1. Assignment modes

Even though NN introduces discontinuities in the temporal development of indoor illuminances, the overall statistical errors for INTERPOLATED and NN are comparable. In case the point of interest is temporarily subject to direct solar illumination, SHADOW TEST outperforms the other two investigated assignment modes. For such cases SHADOW TEST yields reliable simulations of the short-time-step dynamics of indoor illuminances under arbitrary sky conditions. On the other hand, SHADOW TEST should only be employed when needed as it involves additional calculations, because a shadow testing procedure has to be carried out for each considered sunny sky condition. In most real-world design projects INTERPOLATED will be the assignment mode of choice as it quickly yields indoor illuminance

profiles which are reliable under the majority of possible sky conditions. SHADOW TEST should only be used when the appearance of glare due to direct sunlight is investigated.

### 5.2. Accuracies of indoor illuminances

It has been found that the accuracy of SHADOW TEST only slightly depends on the actual blind setting or sky condition. For the desk sensors the magnitude of the MBE and RMSE stayed below 6 and 26% for all blind settings. The ceiling sensors, especially the one near the facade, tend to be harder to simulate as the surrounding landscape cannot be modeled with the necessary detail.

### 5.3. Details of the surrounding landscape

The quality of daylight simulation results decisively depends on whether details of the surrounding landscape are adequately modeled. In this study, modeling the ground in direct vicinity of the facade of the test office proved to be crucial for the accuracy of the simulation results especially for ceiling mounted sensors. The necessity to carefully model the surrounding landscape equally exists for dynamic and static daylight simulations.

### 5.4. Sky model and raytracing errors

The analysis of the ‘scaled’ variant hints that the total simulation errors are caused to roughly equal parts by errors of the sky model and the combined effect of the daylight coefficient method, the raytracing algorithm and the CAD model. The weight of the latter rises if the simulation involves venetian blinds, while the significance of sky luminance distribution model drops with the blinds closed since a growing percentage of the incoming daylight is diffusely reflected from the surrounding ground before entering the test office.

### 5.5. Daylight autonomy and artificial lighting

The results of Sections 4.2 and 4.5 suggest that the annual daylight autonomy for an office featuring external venetian blinds can principally be predicted with an accuracy of a few percentage points. The remaining limiting factor for such precise predictions of the daylight autonomy in a real building are uncertainties of the temporal status of the shading and glare protection devices. The artificial lighting demand can be predicted with a similar accuracy under the same assumptions and if an ideal, automated lighting control system is considered. For a manually operated lighting control system, the complex driving forces which determine how the users of an office influence their working conditions are not well understood as of yet. This issue deserves further attention in the future.

All these findings suggest that dynamic, RADIANCE-based daylight simulation methods which use the concept of daylight coefficients are able to efficiently and accurately

model complicated daylighting elements such as the considered venetian blind system. The extra planning efforts for the architect or lighting engineer for running such a dynamic daylight simulation instead of carrying out a simple daylight factor calculation is limited once the time consuming input of the building model has been accomplished. The additional effort is compensated by additional insight into the lighting situation inside the future building like the prediction of the daylight autonomy and the detection of direct glare and disturbing illuminance variations.

To fully exploit the power of such simulation tools in the daily design process, it is essential to have short-time-step direct and diffuse irradiance input data. Since this data is scarcely available, it will be necessary to implement a model which generates short-term irradiance data from hourly mean values which are widely accessible.

## Acknowledgements

The authors are indebted to their colleagues at the Solar Building Design Group at the Fraunhofer Institute for Solar Energy Systems in Freiburg, Germany. Special thanks to Christian Reise for providing the external irradiance and illuminance data, to Jan Wienold for allowing us to use the test office and to Peter Apian-Bennewitz and Roland Schrengle for helping us with the RADIANCE source code. This work has been sponsored by the German Research Foundation (Deutsche Forschungsgemeinschaft) under the contract number LU 204/10-2.

## Appendix A. Adaptation of ‘rtrace’ for the calculation of daylight coefficients

Minor changes have been made to the output format of the original RADIANCE program *rtrace* to accelerate the calculation of a complete set of daylight coefficients. The raytracing algorithm itself has been left unchanged. Whereas, a regular RADIANCE illuminance simulation yields integral illuminance values due to all light sources in a given scene, the adapted *rtrace*-version provides the contributions due to different light sources separately. With this new feature a complete set of daylight coefficients can be simulated in two *rtrace* runs.

1. To calculate the 148 diffuse and ground daylight coefficients, the building model is placed in a ‘glowing’ sphere of constant luminance. No other light sources are admitted. During the raytracing illuminance contributions are grouped into 148 different bins according to the angular direction under which the backward traced rays hit the surrounding sphere.
2. For the calculation of the direct daylight coefficients, the building model is placed under some 65 angular light

sources with the solar cone opening angle of  $0.53^\circ$ . The positions of the light sources correspond to the representative sun positions of the building site. During the raytracing the illuminance contributions are grouped according to the modifier names of the light sources [6].

The drawback of the adapted *rtrace*-version is that even though the raytracing algorithm itself is identical to the conventional *rtrace*, the required RAM and necessary calculation times rise. The former effect stems from changes made to the caching structure in RADIANCE: during a conventional ambient calculation RADIANCE caches information like the color channel illuminances at already calculated points in the scene to allow for an interpolation or extrapolation of new values from already calculated neighboring points [6]. The adapted *rtrace*-version further stores the illuminance contributions due to all light sources separately, which increases the required memory per cached value by a factor of around 8. The calculation time rises due to the binning procedure by about 30–40%.

## References

- [1] C.F. Reinhart, S. Herkel, The simulation of annual daylight illuminance distributions — a state-of-the-art comparison of six RADIANCE-based methods, *Energy and Buildings* 32 (2000) 167–187.
- [2] G. Ward, F. Rubinstein, A new technique for computer simulation of illuminated spaces, *Journal of the Illuminating Engineering Society* 1 (1988) 80–91.
- [3] P. Tregenza, I. Waters, Daylight coefficients, *Lighting Research and Technology* 15 (2) (1983) 65–71.
- [4] R. Perez, R. Seals, J. Michalsky, All-weather model for sky luminance distribution — preliminary configuration and validation, *Solar Energy* 50 (3) (1993) 235–245.
- [5] R. Perez, P. Ineichen, R. Seals, J. Michalsky, R. Stewart, Modeling daylight availability and irradiance components from direct and global irradiance, *Solar Energy* 44 (5) (1990) 271–289.
- [6] G. Ward, R. Shakespeare, *Rendering with RADIANCE. The Art and Science of Lighting Visualization*, Morgan Kaufmann, Los Altos, CA, 1998.
- [7] J. Mardaljevic, Validation of a lighting simulation program under real sky conditions, *Lighting Research and Technology* 27 (4) (1995) 181–188.
- [8] J. Mardaljevic, Validation of a lighting simulation program: a study using measured sky brightness distributions, in: *Proceedings of the 8th European Lighting Conference*, Amsterdam, 11–14 May 1997, pp. 555–569.
- [9] The measurement station of the Fraunhofer institute for solar energy systems is part of the international daylight measurement (IDMP) network, official website <http://idmp.entpe.fr/>, 1991.
- [10] J. Wienold, A.D. Tenner, L. Zonneveldt, M. Klingler, EULISP — evaluation and user assessment of lighting systems performance, Final Report for the European Commission, Contract No. JOR3-CT95-0016, 1999.
- [11] P. Tregenza, Subdivision of the sky hemisphere for luminance measurements, *Lighting Research and Technology* 19 (1987) 13–14.
- [12] J.-J. Delaunay, Contribution à la modélisation de la lumière naturelle en vue de son application à la simulation de l'éclairage de locaux, Ph.D. thesis at the Université Louis Pasteur de Strasbourg I, 1995.
- [13] G.R. Newsham, Manual control of window blinds and electric lighting: implications for comfort and energy consumption, *Indoor Environment* 3 (1994) 135–144.
- [14] A.D. Tenner, S.H.A. Begemann, G.J. van den Beld, Acceptance and preference of illuminances in offices, in: *Proceedings of the 8th European Lighting Conference*, Amsterdam, 11–14 May 1997, pp. 130–143.